Journal of Physics: Conference Series **160** (2009) 012050 doi:10.1088/1742-6596/160/1/012050

Electronic Calibration of the ATLAS LAr Calorimeter and commissioning with Cosmic Muon Signals

Carolina Gabaldón
Department of Physics, Universidad Autónoma de Madrid, Madrid, Spain
on behalf of the ATLAS LAr Collaboration

E-mail: carolina.gabaldon.ruiz@cern.ch

Abstract. The three cryostats of the Liquid Argon calorimeter System have been gradually installed at their nominal position in the ATLAS cavern from end 2005 to beginning of 2008. After the cabling and installation, calibration runs are taken routinely, allowing to set-up and debug the electronics. Finally cosmic muon runs are also recorded regularly since august 2006 to test *in situ* the signal reconstruction procedure used to obtain the energy in each cell, as well as to check some of the detector performance. This paper presents the current status of these analyses.

1. Introduction

The ATLAS experiment is presently in its last stage of installation in the Point 1 of the Large Hadron Collider (LHC), the last CERN proton-proton collider, and will be complete and ready for the first collisions expected in the autumn 2008. One of the main ATLAS sub-detectors, the Liquid Argon (LAr) calorimeter System, composed of one barrel and two end-cap cryostats, has been gradually installed in its nominal position from the end of 2005 until the beginning of 2008. As a result, it was one of the first systems to start the commissioning phase with regular calibration data taking on its entire coverage. Before 2008, the muon spectrometer trigger was not available and a dedicated trigger set-up, based on the hadronic Tile Calorimeter that surrounds the three cryostats, was developed allowing to record several millions of cosmic muons in the LAr calorimeter system. The muon energy deposit in the calorimeters is generally small and therefore requires a very good understanding of the calibration and the signal reconstruction, especially in its ElectroMagnetic (EM) part. The current status of the cosmic muon analysis is presented, keeping in mind that this provides an unique occasion to test the $\sim$180,000 cells of the full system before the first proton-proton collision.

2. ATLAS LAr Calorimeter System

The ATLAS LAr Calorimeter System is composed of three sampling calorimeters with Liquid Argon (*LAr*) as sensitive material, covering a pseudorapidity region $|\eta| < 4.9$: the ElectroMagnetic Calorimeter in $|\eta| < 3.2$, the Hadronic EndCap Calorimeter (HEC) in $1.5 < |\eta| < 3.2$ and the Forward Calorimeter (FCal) in $3.1 < |\eta| < 4.9$.

The EM calorimeter is a device based on an accordion shape geometry consisting of lead absorbers and electrodes coupled to a fast electronic integration. This allows to combine the robust and very well

tested liquid argon technology, with a perfect azimuthal hermeticity and a clean signal extraction in the harsh LHC environment. The EM calorimeter is divided in one barrel, covering $|\eta| < 1.475$ and two end-caps, $1.375 < |\eta| < 3.2$. In depth, three very granular compartments (S_1, S_2, S_3) allow a detailed measurement of the electron and photon EM shower lateral and longitudinal development (Figure 1). This is particularly usefull at LHC to separate efficiently electrons from jets and photons from π_0's. A presampler device is added in the most critical region for the amount of material upstream the EM calorimeter ($|\eta| < 1.8$) and allows to recover the electron/photon energy lost in the material in front (inner detector, cryostat and solenoid coil up to $|\eta| < 1.5$). As a result, the total number of read-out channels or cells is about $170,000$, typically an order of magnitude above the calorimeters used in the Tevatron experiments. A smooth operation of all these cells together represents a major challenge needed for example to achieve the foreseen ATLAS Higgs discovery potential in the two photon Higgs decay channels.

The HEC uses the Cu-LAr sampling plate technology with "cold" preamps mounted on the calorimeter. It is designed to measure the jet energy escaping the EM calorimeter and therefore a coarser granularity, corresponding to the level one calorimeter trigger tower, is used. Finally, the FCal is a copper-tungsten/LAr detector which covers the region closest to the beam. It provides a hermetic calorimeter system up to $|\eta| < 4.9$ with more than 10 units of interaction length λ. The segmentation of the Liquid Argon System is recalled in Table 1. More details on its commissioning and installation can be found in Ref. [1].

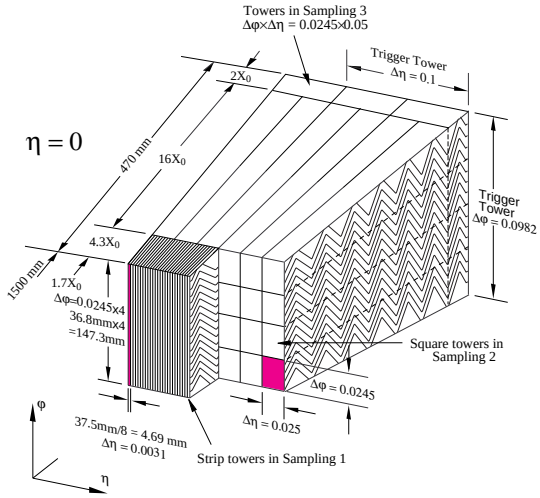

Figure 1. Sketch of the accordion and sampling structure of the EM Calorimeter.

Table 1. Covered region and number of read-out channels of the sub-detectors of the Liquid Argon System.

LAr detector	Channels	Region
EM calorimeter	173312	$\|\eta\| < 3.2$
HEC	5632	$1.5 < \|\eta\| < 3.2$
FCal	3524	$3.1 < \|\eta\| < 4.9$

3. Signal reconstruction with the EM Calorimeter

The LAr calorimeter signal is generated by the drift of the ionization electrons in the electric field provided by the High Voltage (HV) in the LAr gap. The ionization current has a triangular shape, where the peak is proportional to the energy deposited by the shower. The ionization signal is pre-amplified and then shaped by a $CR - RC^2$ bipolar filter at the end of the readout chain. The bipolar signal is sampled every 25 ns (the LHC bunch crossing period) and 5 samples are digitized and used in the signal reconstruction procedure. For special runs, like the ones with cosmic muons, more than 5 samples are digitized and recorded (typically 25 or 32). Figure 2 shows a comparison between the original triangular signal generated inside the LAr gap and the output signal after passing the readout electronics. The maximum has been normalized to 1. The bipolar shaper is designed such that the maximum of the

triangular signal corresponds to the maximum of the shaped pulse. Hence, the maximum amplitude of the shaped pulse is proportional to the energy deposited by the ionizing particles in the readout cell.

Starting from the digitized samples, two relevant quantities are deduced with a digital filtering technique called Optimal Filtering [2]: the signal maximum amplitude (A_{max}) and the difference between the assumed and reconstructed time (Δt). The inputs to the method are: i) the covariance or autocorrelation matrix of the samples, which contains the noise information, ii) the predicted pulse shape (g^{phys}), and iii) its first derivative (dg^{phys}/dt). The outputs of the method are the weights $a_i,\ b_i\ \ i=1,\ldots,n$ (n is the number of samples) which allows to reconstruct A_{max} and Δt as :

$$A_{max} = \sum_{i=1}^{n} a_i (S_i - p), \qquad \Delta t = \frac{\sum_{i=1}^{n} b_i (S_i - p)}{A_{max}} \tag{1}$$

where $S_i\ \ i=1,\ldots,n$ are the 25 ns samples and p is the pedestal level of a given readout cell (both in ADC counts). Thanks to the autocorrelation matrix, the noise contributions to the signal are minimized. Two sources of noise are foreseen in the calorimeter during operation at LHC: the electronic noise and the pile-up noise. Since this article refers to cosmic muon data, only the first source of noise enters in the analysis.

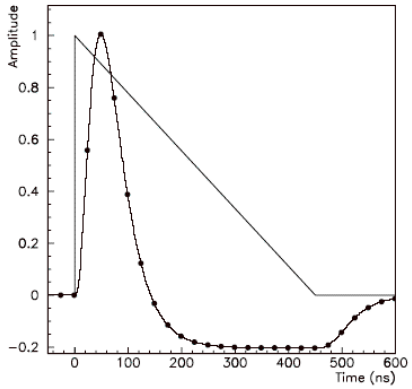

Figure 2. Ionization signal (a) and shaped signal at the end of the readout chain (b).

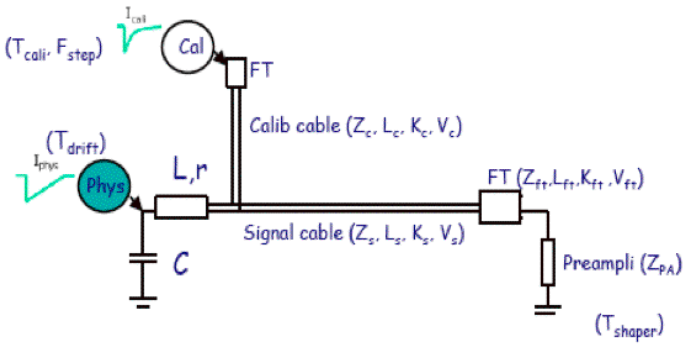

Figure 3. Schematic model of the readout chain of the LAr EM calorimeter cells.

To determine the Optimal Filtering Coefficients for each calorimeter cell the most difficult step is to predict the pulse shape of the physics signal. This can be done thanks to the calibration system, that sends a well-known exponential signal on the cold electronics which then follows the same readout path as the physics one (Figure 3). Two methods have been developed in the electromagnetic calorimeter. The first one, presently used to commission the detector [3], where the cell response to a calibration pulse shape is used to predict completely the physic pulse shape. And an alternative method [4], that uses an analytical model of the EM readout to predict the physic pulse shape per cell. In this last approach, all the circuits parameters are measured, except two, left free in order to match the measured calibration pulse response. A similar method is used in HEC [5], whereas FCal uses the physics pulse extracted from test beam data for the prediction [6].

Once the amplitude has been determined, the energy of each cell is then computed as:

$$E = F_{gain} \times \frac{1}{F_{I/E}} \times A_{max} \tag{2}$$

where F_{gain} is the electronic gain, converting the signal amplitude from ADC to current and $F_{I/E}$ is the absolute energy scale.

4. Commissioning of the ATLAS electromagnetic calorimeter with cosmic muons

The analysis of cosmic muon events is the only way to test the EM calorimeter *in situ* with physics signals before LHC collisions. The process of integrating more and more sub-systems has been ongoing since summer 2006. During the summer 2007, the situation for the EM barrel and one EM end-Cap liquid Argon calorimeters was stable and the cosmic data were taken nearly every weekend.

A dedicated trigger using only Tile calorimeter signals was configured to cope with the absence of the muon spectrometer trigger. Figure 4 shows the Tile towers (One trigger tower is the sum of all Tile cells in a region of $\Delta\eta \times \Delta\phi = 0.1 \times 0.1$) that were included in the trigger for the data taking.

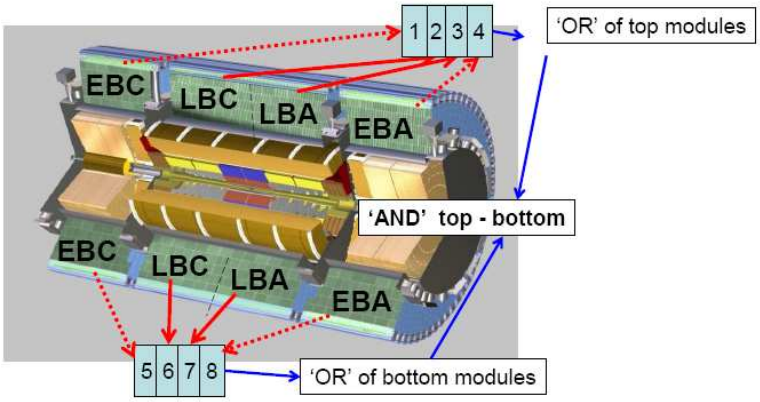

Figure 4. Tile trigger setup and logic of the top-bottom coincidence. Tile modules are labeled LB in the central part and EB in the end-cap part. A and C refer to $z > 0$ and $z < 0$ respectively.

Cosmic muons can be classified in two categories: the ones which radiate bremmsstralung photons and the ones behaving as Minimum Ionizing Particles (MIP). In the first case, high energy deposits can be selected ($E > 500$ MeV) to check the quality of the predicted physics signal. Note, that this is the only option for the EndCaps due to the absence of projective muons, i.e. muons pointing to the nominal Interaction Point [7]. In the second case, which corresponds to 99% of the events, a coarse check of global uniformity, both for (η,ϕ) spatial coordinates and for timing, is possible for the EM barrel calorimeter [8]. For these studies, projective or quasi-projective muons are required.

4.1. Studies with high energy muons

To compare the predicted physics pulses (g_i^{phys} normalized to one) with the data, the prediction must first be adjusted in time, to take into account the asynchronous muon arrival times, and in amplitude by multiplying g_i^{phys} by A_{max} computed with Equation (1). After this step, Figure 5 shows typical physics shapes for middle sampling (S2) in the EM barrel (left) and in the EM end-cap (right). The predictions agree nicely with the data in the raising and falling edges of the pulses. A similar comparison can be made with the other LAr detectors (Figure 6) that also shows a good agreement between the data and the predicted physic shape.

To perform a systematic quantitative comparison between data and pulse shape predictions over the full η coverage the following χ^2 can be computed:

$$\chi^2 = \sum_{i=1}^{n=5} \left(\frac{S_i - A_{max} * g_i^{phys}}{\sigma_{noise}} \right)^2 \qquad (3)$$

where S_i is the amplitude of each sample i in ADC counts for data and σ_{noise} corresponds to the noise for a single sample in ADC counts.

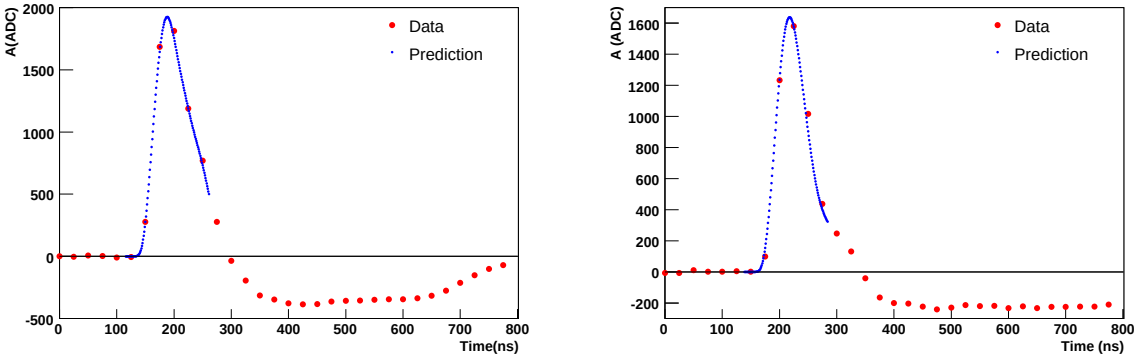

Figure 5. Typical cell response to high energy deposits in the EM barrel (left) and EM endcap (right).

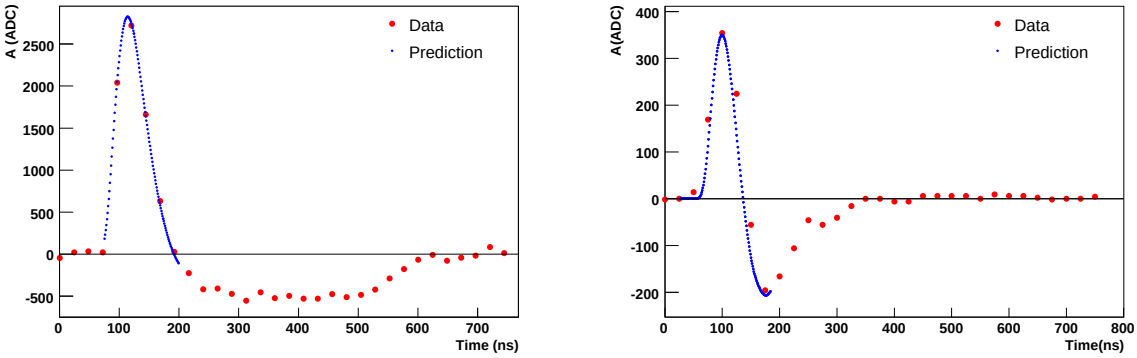

Figure 6. Example of cell response to cosmic signal in HEC (left) and FCal (right).

By construction, the χ^2 of Equation (3) depends on the square of the reconstructed amplitude A_{max} (the error on the predicted pulse shape can not be estimated) [9]. Therefore, an η – independant estimator, Q, of the prediction quality is build when dividing by ${A_{max}}^2$. Figure 7 shows this estimator as a function of the energy for the middle layer in the EM barrel (left) and in the EM end-cap (right). Its dependence with energy can be fitted by the following simple function :

$$Q = \frac{\chi^2}{n_{samples} \times {A_{max}}^2} = \frac{p_0}{E^2} + p_1 \tag{4}$$

The first term, dominating at low energy, is due to the gaussian noise fluctuation for each sample. The second term, dominating at high energy, reflects the quality of the predicted shape as compared with the data. The results are only slightly better in the EM barrel compared to the EM end-cap. This is the first proof of the quality of an ATLAS-like signal reconstruction in the EM end-caps, despite its more challenging geometry: the LAr gap varying with η from 3 mm to 1 mm whereas it is 2 mm everywhere in the EM barrel. This is also illustrated in Figure 8, which shows the pulse shape prediction quality Q as a function of η. These results are obtained by applying a lower energy cut (1.5 GeV in S2), to minimize the noise contribution, and an upper cut (2500 ADC counts) to avoid high gain saturation. This assesses the coherence of the signal reconstruction quality, using 5 samples as foreseen in ATLAS, over the complete EM calorimeter coverage $0 < |\eta| < 3.2$.

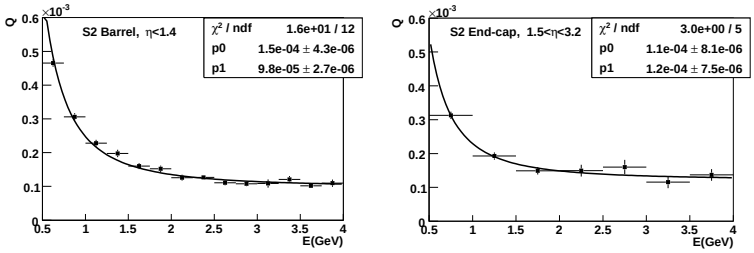

Figure 7. Estimator of the quality of the predicted physics pulse shape as a function of the energy in S2 cells of the EM barrel (left) and of the EM end-cap (right).

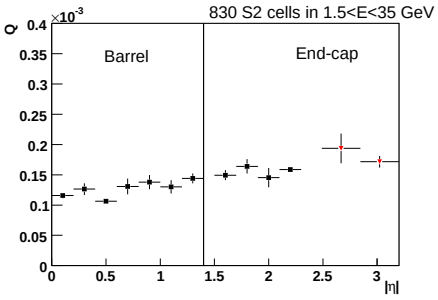

Figure 8. Estimator of the quality of the predicted physics pulse shape as a function of $|\eta|$ for S2.

4.2. Studies with MIP cosmic muons

In the previous section the quality of the standard signal reconstruction was tested with high energy muons. The following step is to extract a high quality sample of MIP cosmic muons to perform a global check of the EM calorimeter performance.

The two main difficulties in this analysis come from the small energy deposit of a MIP in the EM calorimeter (300 MeV in a S2 cell) and the non projectivity of cosmic muons. In the first case, the full noise reduction capability of the signal reconstruction method can be used (see section 3). As an example, Figure 9 shows that the signal to noise can be improved by a factor > 2 when considering 25 samples instead of 5. In order to extract a pure "projective" muon sample passing close to the nominal interaction point, a dedicated algorithm has been developed to reconstruct cosmic muon trajectories. The trajectory is extracted by fitting with a straight line the position of Tile cells in the top-bottom side (Figure 10). Only muons which pass within ± 30 cm of the interaction point in the $Y = 0$ plane are selected, representing $10,000$ events.

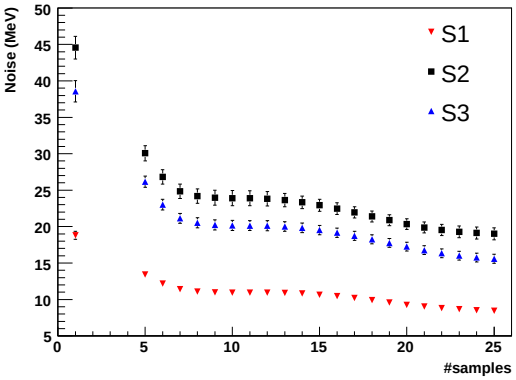

Figure 9. Noise as a function of the number of samples used by optimal filtering for EM calorimeter layers in high gain.

The first task to be performed with the LHC data is the timing of the calorimeter. Figure 11 shows the reconstructed EM time versus the reconstructed Tile time corrected for time of flight at $Y = 0$. A linear correlation between the EM cell time and the Tile time is observed. After fixing the slope to be unity in the linear fit, the error on the y-intercept decreases to just below 1 ns. The collection of this timing offsets allows for a first look at timing uniformity.

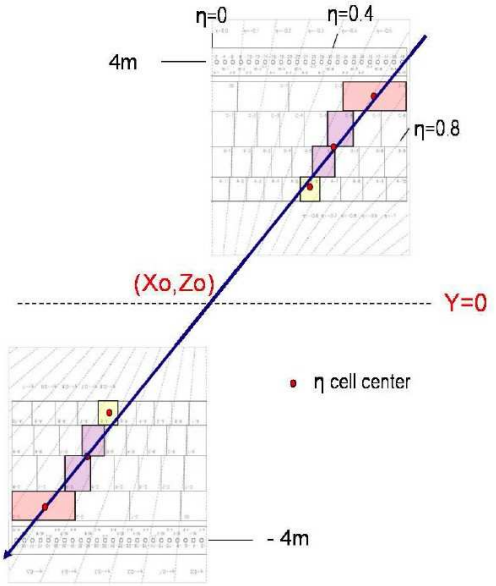

Figure 10. Schematic description of a reconstructed muon track. $Y = 0$ represents the horizontal plane with the interaction point (X_0, Z_0) in.

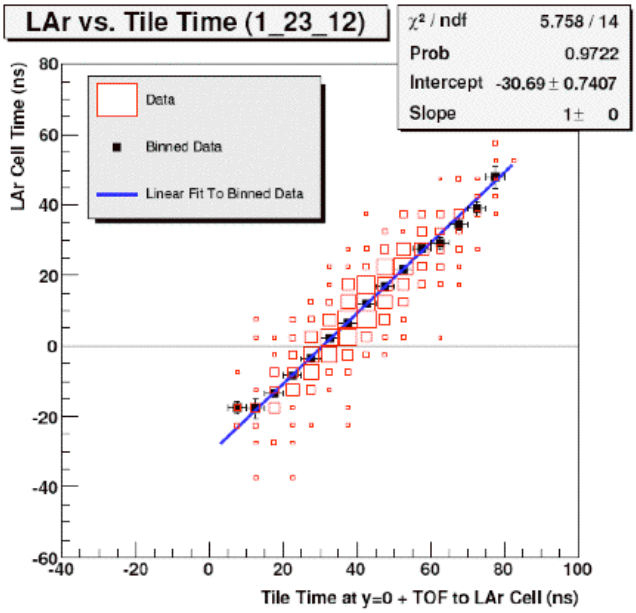

Figure 11. EM cell time vs. Tile Time at $Y = 0$ corrected for time of flight.

Cosmic muons also provide a good opportunity to study the calorimeter response, with more modules than in the test beam, before the start of the LHC. After a projective requirement their energy depositions should follow a Landau distribution. This is illustrated in Figure 12 which displays the measured energy distribution for clusters of $\Delta\eta \times \Delta\phi = 3 \times 3$ cells in the range $0.3 < |\eta| < 0.4$. The χ^2/NDF strongly supports the choice of a Landau convoluted with a Gaussian as the fit function which describes the data. The fitted value of the Gaussian width parameter, $\sigma_G = 60$ MeV, corresponds to the uncorrelated noise contribution of 9 cells ($20 \times \sqrt{9} = 60$ MeV) .

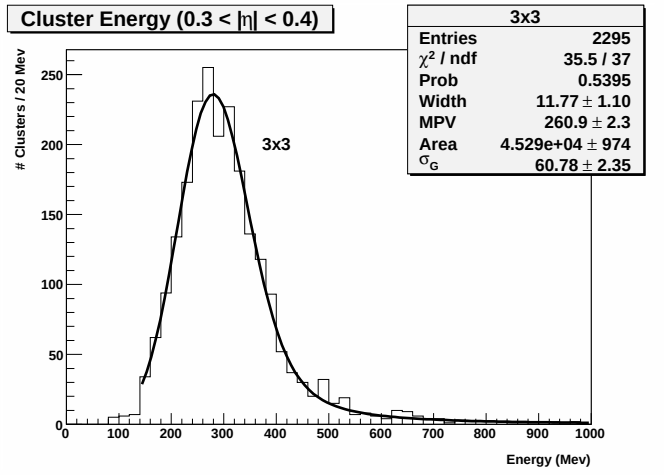

Figure 12. Measured 3×3 cluster energy distributions in the range $0.3 < |\eta| < 0.4$, using the $(|X_0|, |Z_0|) < (30$ cm, 30 cm) projectivity selection criteria for data.

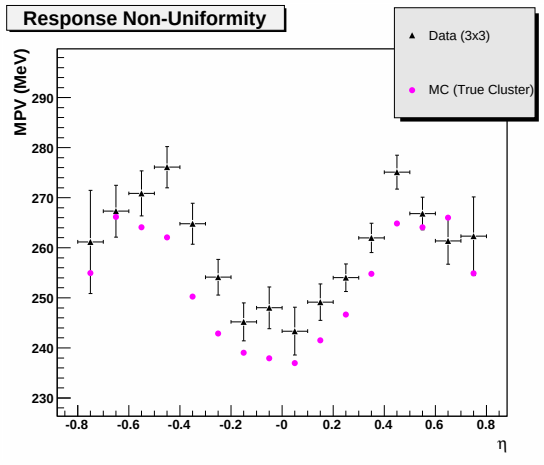

Figure 13. Most probably energy value vs η for 3×3 cluster (black triangle) and MC true clusters (pink circle).

Figure 13 presents the most probable value (MPV) as determined from the fits of the energy distributions binned in η intervals with a width of 0.1 for $|\eta| < 0.8$. The dependence of the MPV on η is compared to the true cluster values found in the MC analysis corresponding to the same event selection. The η dependence of the data is in good agreement with the MC simulation at the level of 3%. To probe the true detector non-uniformity for individual cells at the level of 1% would require approximately $160,000$ projective events, which is out of reach before the LHC start.

Conclusions

At present, ATLAS is completely installed in its final position in the Point 1 cavern. The ATLAS Liquid Argon System was one of the first to begin the installation in 2006. These two years were an occasion to exercise the electronics calibration and assess the robustness of the signal reconstruction in all LAr detectors. Since October 2006, cosmic data have been collected nearly every weekend. This allows a full-scale test of the signal reconstruction chain which is now understood at 1% level. Despite the small and mostly non-projective signals, cosmic muons provide a first in situ test of LAr detectors. A first check of the overall energy scale has been shown to agree with simulation to within 3% for typical cosmic energy depositions.

All these results give confidence that the LAr system will be ready to take data in autumn 2008 when the first LHC pp collisions will occur.

Acknowledgments

The work presented here has been performed within the ATLAS LAr collaboration. This analysis would not have been possible without the dedicated effort of many people in our LAr detector group and the ATLAS collaboration over many years. I'm especially indebted to those who built, integrated and installed the LAr detectors in the ATLAS cavern, and those who operate the detector on a daily basis.

References

[1] H. Wilkens, these proceedings.
[2] W.E. Cleland et E.G. Stern, *Signal processing considerations for liquid ionization calorimeter in a high rate environment*, Nucl. Inst. Meth. **A 338** (1994) 467.
[3] D. Banfi, M. Delmastro and M. Fanti, *Cell response equalization of the ATLAS electromagnetic calorimeter without the direct knowledge of the ionization signals*, SN-ATLAS-2005-054, J. Inst **1** (2006) P08001.
[4] C. Collard *et al.*, *Prediction of signal amplitude and shape for the ATLAS electromagnetic calorimeter*, ATL-LARG-PUB-2007-010.
[5] C. Cojocaru, *Hadronic calibration of the ATLAS Liquid Argon End-Cap Calorimeter in the Pseudorapidity Region 1.6 $< \eta <$ 1.8 in Beam Tests*, NIM A531 (2004) 481-514.
[6] J.P. Archambault *et al.*, *Energy calibration of the ATLAS Liquid Argon Forward Calorimeter*, JINST 3 P02002.
[7] C. Gabaldon Ruiz, M. Kuna et al., *et al.*, *Signal reconstruction in the EM end-cap calorimeter and check with cosmic data in the region* $0 < \eta < 3.2$, ATLAS note ATL-LARG-PUB-2008-001.
[8] M. Cooke, P.S. Mangeard, M. Plamondon *et al.*, *In situ commissioning of the ATLAS electromagnetic calorimeter with cosmic muons*, ATLAS note ATL-LARG-PUB-2007-013.
[9] M. Delmastro, *Quality factor analysis and optimization of digital filtering signal reconstruction for liquid ionization calorimeters*, NIMA-D-08-00417.